

HMOX1 as a Novel Biomarker for Glucose–Lipid Metabolism Disorder and T2DM: Systematic Bioinformatics Investigation and Experimental Verification

Qi Xu, Hongrong Zhang,^{||} Nuobing Ruan,^{||} Jiawen Jing, Yufan Li, Jindong Zhao,* and Zhaohui Fang*



Cite This: *ACS Omega* 2025, 10, 16123–16137



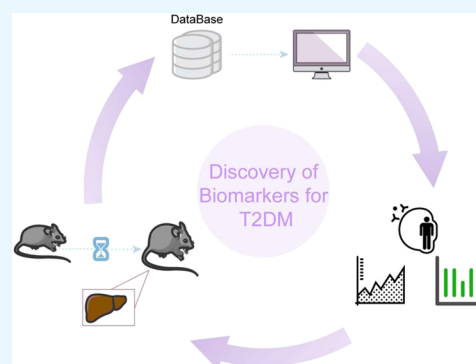
Read Online

ACCESS |

Metrics & More

Article Recommendations

ABSTRACT: Type 2 diabetes mellitus (T2DM) has led to a considerable increase in morbidity and mortality worldwide. Current treatments control blood glucose but cannot reverse the disease, making it important to identify biomarkers that predict T2DM onset and progression. This study explores heme oxygenase 1 (HMOX1) as a novel biomarker for T2DM through bioinformatics and experimental validation. Core differentially expressed genes (DEGs) were identified using the Gene Expression Omnibus database, with Gene Ontology, Kyoto Encyclopedia of Genes and Genomes, and Gene Set Enrichment Analysis analyses revealing notable pathways, including Toll-like receptor signaling and cytokine receptor interactions. A Nomogram model and receiver operating characteristic curves demonstrated strong diagnostic effectiveness for these core DEGs. The CIBERSORT algorithm assessed the relation between core DEGs and immune cell infiltration, showing substantial associations with several immune cell types, particularly highlighting HMOX1's correlation with eight immune cells ($p < 0.05$). In a mouse model, db/db mice displayed typical diabetic characteristics and lower serum HMOX1 levels compared to db/m controls ($p < 0.01$). Histological analysis confirmed liver damage and decreased expression of NFE2L2 and HMOX1 in diabetic mice tissues ($p < 0.05$). HMOX1 is identified as a promising biomarker for T2DM, with its downregulation confirmed through bioinformatics and experimental methods.



1. INTRODUCTION

Type 2 diabetes mellitus (T2DM) has emerged as a notable global health challenge, characterized by increasing incidence and mortality rates.¹ While mortality from certain non-communicable diseases, such as chronic respiratory ailments and cardiovascular diseases, has declined, diabetes-related deaths have steadily increased from 2000 to 2019.² The “World Health Statistics 2023” report by the WHO indicates that T2DM now ranks among the leading causes of disability-adjusted life years, particularly in the Americas, where it has surpassed stroke.³

The etiology of T2DM is multifaceted, encompassing genetic predispositions, lifestyle factors, and psychosocial influences.⁴ Current therapeutic options include oral medications like metformin, sulfonylureas, and DPP4 inhibitors, along with injectable insulin and GLP1 receptor agonists.^{5–7} While these interventions effectively control blood glucose levels, they do not reverse the underlying progression of diabetes, especially in later stages. This limitation underscores the need for reliable biomarkers that can predict the onset of T2DM and facilitate early intervention strategies.

Biomarkers are measurable indicators at the molecular or cellular level that provide insights into disease processes and enhance risk assessment strategies.^{8,9} Their applications span

various fields;¹⁰ for instance, markers like EIF4G1¹¹ and NUSAPI¹² have been associated with cancer progression, while other specific proteins, such as p-tau231, are emerging as potential indicators of neurodegenerative diseases such as Alzheimer's Disease.¹³ Biomarkers signify early events in disease initiation and can serve as predictive indicators. Establishing the links between disease and biomarkers enables early detection and prognosis.

Traditional biomarkers for diagnosing T2DM generally include blood glucose, glycosylated hemoglobin, and insulin function.¹⁴ However, they are of limited use in risk assessments for early diabetes and complications due to high false-positivity and complex testing that precludes large-scale screening.^{15–17} Recent research has focused on identifying new biomarkers with clinical value in T2DM to improve early diagnosis, treatment, and disease monitoring.

Received: October 23, 2024

Revised: February 11, 2025

Accepted: April 11, 2025

Published: April 16, 2025



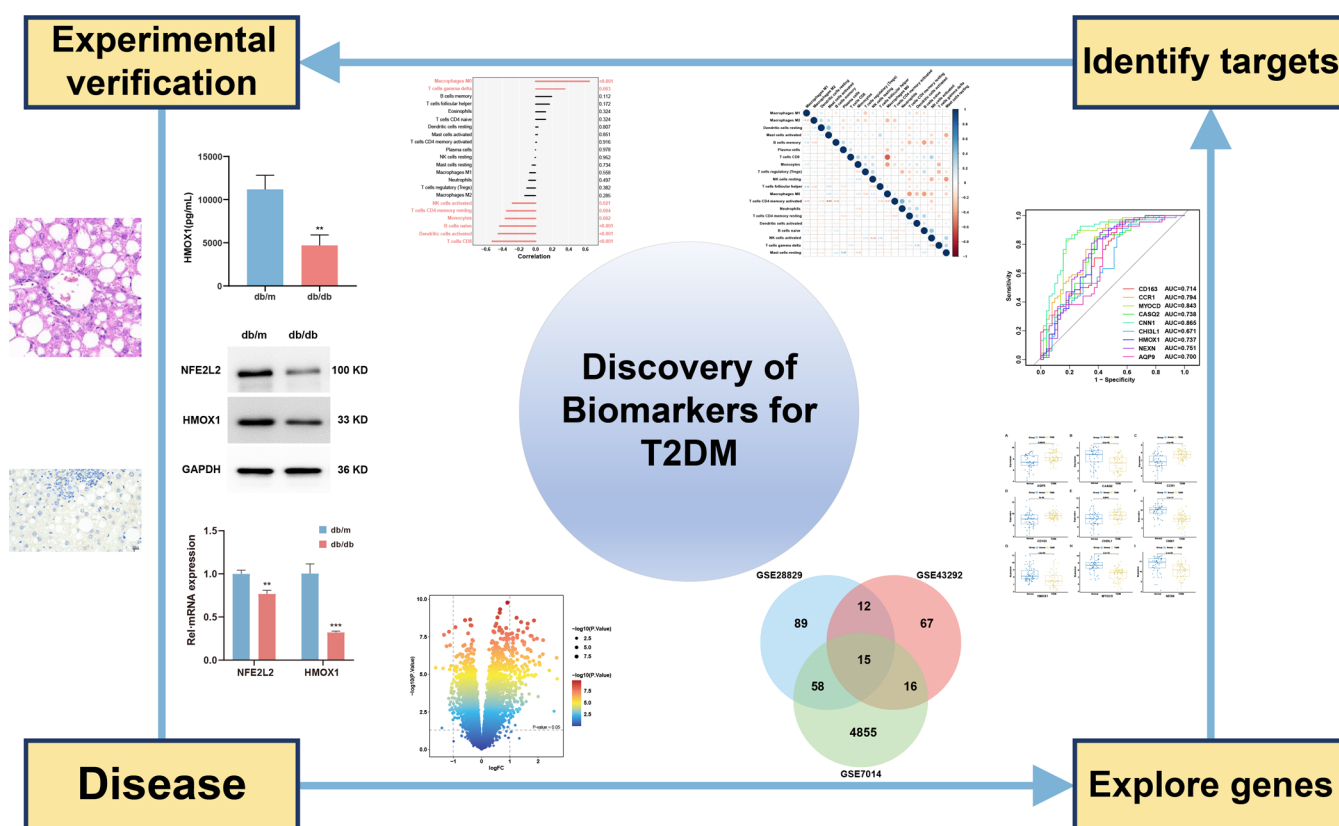


Figure 1. Research framework for T2DM biomarkers.

Heme Oxygenase 1 (HMOX1) catalyzes the oxidative degradation of heme groups in hemoglobin, myoglobin, and cytochrome p450. It and its enzymatic products have anti-inflammatory functions and regulate homeostasis, immune function, and host defense.¹⁸ Inflammation has evolved into a key determinant of diabetes and its major complications. Persistent hyperglycemia causes metabolic, vascular, and nerve damage, leading to vascular and neurological complications.¹⁹ On the one hand, oxidative stress-induced damage to pancreatic β -cells and target tissues can be alleviated by HMOX1 through its antioxidant effects, thereby contributing to the maintenance of pancreatic function and the improvement of insulin sensitivity.²⁰ On the other hand, a significant role of HMOX1 has been identified in the regulation of immune cell function and inflammatory responses. Studies have suggested that macrophage phenotypes within tissues can be modulated by HMOX1, leading to a decrease in tumor necrosis factor- α and interleukin-6 levels in inflammatory diseases.²¹ Furthermore, the upregulation of HMOX1 has been suggested to contribute to the improvement of the chronic inflammation in T2DM.²² HMOX1 binds nuclear factor erythroid 2-related factor 2 (NFE2L2) in response to oxidative damage and participates in the restoration of cellular homeostasis via the AKT/NFE2L2 pathway, reducing the expression of inflammatory factors while inducing the expression of anti-inflammatory, antioxidative, and proangiogenic factors.^{23–25} Given the close relationship between HMOX1 and T2DM, coupled with its significant role in oxidative stress and inflammatory responses, the potential of HMOX1 as a biomarker for T2DM is emphasized. The expression level of HMOX1 may reflect the status of oxidative stress and inflammation severity in T2DM patients, thereby

providing a potential approach for early diagnosis, monitoring disease progression, and assessing treatment response.

Herein, we report our investigation of HMOX1 as a novel biomarker for T2DM through a combination of bioinformatics analysis and empirical validation. Core differentially expressed genes (DEGs) associated with T2DM were identified via the Gene Expression Omnibus (GEO) database. Gene Ontology (GO), Kyoto Encyclopedia of Genes and Genomes (KEGG), and Gene Set Enrichment Analysis (GSEA) revealed substantial associations with inflammatory pathways, and a nomogram model combined with receiver operating characteristic (ROC) curves was used to assess the diagnostic accuracy of the core DEGs. These in silico studies were followed by validation studies in animal experiments. We discuss these results and the potential utility of HMOX1 as a biomarker for predicting the onset of T2DM (Figure 1).

2. MATERIALS AND METHODS

2.1. Data Set Construction. To improve the generalizability of the study, we combined multiple data sets, known as cohorts A, B, and C. The data sets originated from the GEO (<https://www.ncbi.nlm.nih.gov/geo/>). Cohort A (GSE7014) comprises 6 normal and 20 disease samples, cohort B (GSE28829) comprises 13 normal and 16 disease samples, and cohort C (GSE43292) comprises 32 normal and 32 disease samples. The data sets produced platform files that converted probes into gene symbols for analysis.

2.2. Identification of DEGs. DEGs between the experimental and control groups were identified using the limma package in R software (version 4.3.0) to screen cohorts A, B, and C. First, the data were processed by $\log_2(x + 1)$ transformation and normalization using the “normalizeBetween-

nArrays" function. The filtering threshold of cohorts A and B was $\log \text{FCI} > 1$, with adj- p -value < 0.01 . For cohort C, the filtering condition was $\log \text{FCI} > 1$, and adj- p -value < 0.05 . Volcano plots were generated using the ggplot2 package. The x-axis of the volcano plot represents \log_2 fold change ($\log_2 \text{FC}$) in gene expression. Positive and negative $\log_2 \text{FC}$ values represent upregulation and downregulation, respectively.

2.3. Hub Genes Determination and PPI Network Construction. We initially used the "VennDiagram" package in R software to identify common genes among DEGs in each cohort to identify the difference-related hub genes. The protein–protein interaction (PPI) network for the hub genes was constructed using the STRING database with the minimum required interaction score set at 0.4. Network visualization was performed in Cytoscape. In the PPI network, nodes represent hub genes, and the edges represent the relationships between hubs. Degree, an important topological parameter, was analyzed using the CytoHubba plugin within Cytoscape to evaluate network centrality and identify the hub genes. A greater degree correlates with a greater hub importance.

2.4. GSEA. GSEA was utilized to investigate the potential mechanisms of core genes and examine whether each core gene was enriched in significant biological processes. GSEA is a widely used computational method for determining whether genes differ significantly between biological states. T2DM patients were categorized into high-risk and low-risk groups based on median risk scores. We used the "clusterProfiler" package to perform GSEA analysis on the core high- and low-expression genes. The gene sets c5.go.v7.4.symbols.gmt and c2.cp.kegg.v7.4.symbols.gmt were selected as the reference sets. Functional or pathway terms with p -values < 0.05 were deemed statistically significant, and plots were generated using "gseaplot."

GO functions and KEGG pathway analyses were performed on the core gene set, and an enrichment analysis network was constructed using Metascape. The enrichment results were visually represented using ggplot2.

2.5. Construction of the Risk Prediction Model for T2DM. To explore the influence of genes on patient survival outcomes, ROC curves were constructed using the "ROC" package to evaluate the effectiveness of the model as a diagnostic criterion. The prognostic ability and effectiveness of the model were measured by calculating the area under the ROC curve (AUC). $\text{AUC} > 0.5$ is considered statistically significant.

To explore the prognostic role of the core genes, a nomogram model was built using the "rms" package to predict the risk of T2DM. Harrell's concordance index was used to evaluate the model performance of the nomogram. The correlation between genes and overall survival (OS) was determined using regression models. Furthermore, calibration curves demonstrated the predictive accuracy of OS.

2.6. Immune Cell Analysis of the Risk Prediction Model. To explore the role of immune cells in T2DM, the CIBERSORT algorithm was used to evaluate the infiltration levels of 22 immune cell types, including dendritic cells, macrophages, neutrophils and B cells. CIBERSORT, a deconvolution algorithm based on standardized gene expression profiles, can be used to quantify immune cell composition, greatly expanding the potential utility of genomic databases.

Assessing immune cell expression levels against the prognostic model by correlation analysis revealed significant predictive strength in T2DM. The relationships between the prognostic model and immune cell expression were depicted using the "limma," "ggpubr," and "ggExtra" packages.

2.7. Experimental Animal Preparation. Ten C57BLKS/J-LepR(db/db) mice with genetic T2DM and 10 healthy controls (db/m), aged 8 weeks, were purchased from Beijing Viewsolid Biotechnology (Beijing, China). All mice were maintained under standard conditions of maintenance diet, room temperature (20–25 °C), relative humidity 45–55%, and 12-h light/dark cycle. After 12 weeks, the mice were sacrificed, and tissue and blood samples were collected.

All animal procedures were approved by the Institutional Animal Ethics Committee (Approval No: VS2126A-00143). Animal use and care were performed per the Guide for the Care and Use of Laboratory Animals.

2.8. Related Indicators. **2.8.1. Body Weight.** After 1 week of acclimatization, the mice were weighed on an electronic balance (BW). From the start of feeding, BW was recorded every 2 weeks.

2.8.2. Fasting Blood Glucose. Mice were fasted for 12 h in advance, and fasting blood glucose (FBG) levels were measured using an active-type glucometer (CONTOUR PLUS) after blood collection from the tip of the tail using a disposable blood sampling needle. Measurements were made every 2 weeks.

2.8.3. Blood Biochemistry. Blood was collected from the eye after the animals were anesthetized. After being left to stand at room temperature for 2 h, the serum was obtained by centrifugation at 1500g, 4 °C for 15 min. Serum glucose, total cholesterol (TC), and triglyceride (TG) levels were measured using a fully automated biochemical analyzer and commercial reagents. Serum fasting insulin (FINS), high-density lipoprotein-cholesterol (HDL-C), low-density lipoprotein-cholesterol (LDL-C), glycosylated hemoglobin (HbA1c), and heme oxygenase (HMOX1) were detected using ELISA kits. Insulin resistance (IR) was assessed using the HOMA-IR model as follows

$$\text{HOMA-IR} = \frac{\text{FBG (mmol/L)} \times \text{FINS } (\mu\text{U/mL})}{22.5}$$

2.8.4. Histopathology and Immunohistochemical Staining. Fresh liver tissues were fixed in 4% paraformaldehyde for 48 h and then dehydrated with gradient ethanol. The tissues were paraffin-embedded after being transparentized with xylene and soaked in wax for 4 h. The embedded tissues were sectioned (4 μm) on a microtome. The sections were spread on glass slides in warm water (40 °C), oven-dried (60 °C), and stored at room temperature.

The sections were soaked in xylene and deparaffinized in gradient ethanol to water for H&E staining. The sections were stained with Harris hematoxylin for 10 min, differentiated in 1% hydrochloric alcohol for 10 s, and returned to blue in 0.6% ammonia, with running water washes between each step. The sections were stained in eosin for 3 min, dehydrated with gradient ethanol, dried in xylene, and sealed with neutral gum.

Paraffin sections were deparaffinized with xylene and gradient ethanol to water and then immersed in antigen repair buffer in EDTA by microwave heating. After washing with PBS, 3% hydrogen peroxide solution was added dropwise and blocked at room temperature for 25 min. The sections were incubated with 3% BSA for 30 min at room temperature,

followed by dropwise addition of primary antibody NFE2L2 (1:200, Bioss) and HMOX1 (1:400, ABclonal) diluted with 3% BSA overnight at 4 °C. The corresponding secondary antibodies were added and incubated for 50 min at room temperature. Next, DAB was added dropwise to the sections for color development, and hematoxylin was counterstained for 10 min, followed by dehydration, transparency, and sealing. Nuclei were stained blue, and positive protein expression is indicated by tan stain.

Sections were observed by light microscopy, and 3–5 fields of view were randomly recorded.

2.8.5. Quantitative Real-Time Polymerase Chain Reaction (qPCR). Total RNA from mice liver tissue was extracted using TRIzol reagent, and concentration/purity was measured spectrophotometrically. The mRNA was reverse-transcribed into cDNA using a kit, and qPCR was performed on a CFX Connect thermal cycler (Bio-Rad). The reaction conditions consisted of an initial incubation at 95 °C for 30 s, followed by 40 cycles of 95 °C for 10 s, 56 °C for 30 s, and 72 °C for 30 s. The melting curve analysis was performed under the conditions of 95 °C for 15 s, 60 °C for 60 s, and 95 °C for 15 s. The relative expression level of the target gene was calculated using the $2^{-\Delta\Delta C_t}$ method with GAPDH as a reference. The primers were synthesized by SANGON Biotech (Table 1).

Table 1. Primer Sequences

primer	sequence (5'–3')	length	amplicon size (bp)
NFE2L2	F: TCTTGGAGTAAGTCGAGAAGTGT	23	140
	R: GTTGAACTGAGCGAAAAAGGC	22	
HMOX1	F: AAGCCGAGAATGCTGAGTTCA	21	100
	R: GCCGTGTAGATATGGTACAAGGA	20	
GAPDH	F: AGGTCGGTGTGAACGGATTG	21	123
	R: TGTAGACCATGTAGTTGAGGTCA	23	

2.8.6. Western Blot Analysis. Liver tissue samples (100 mg) were minced, lysed, and ground in a precooled ball mill. After centrifugation at 4 °C and 14,000g for 5 min, the supernatant was isolated, and the protein concentration was determined using the BCA method. Protein loading buffer (5×) was added and heated in a 100 °C water bath for 10 min. The proteins were separated by SDS–PAGE and transferred to a PVDF membrane. After blocking in 5% BSA for 2 h at room temperature, the membrane was incubated overnight incubation with primary antibodies NFE2L2 (1:5000, ABclonal), HMOX1 (1:1000, Zenbio), GAPDH (1:10,000, Proteintech) diluted with 3% BSA at 4 °C. The membrane was washed and then incubated with the corresponding secondary antibodies HRP-Goat antirabbit and HRP-Goat antimouse (1:50,000, Seracare) diluted with 3% BSA at room temperature for 2 h. The developing solution was added dropwise, and the membrane was exposed on a photoimager. Signal intensity was quantified using ImageJ and normalized to GAPDH.

2.9. Statistical Analysis. Statistical analysis and visualization for the bioinformatics analysis were carried out using R software (version 4.3.2). SPSS 26.0 was used for statistical analysis. Data are presented as means \pm standard errors. Univariate analysis was used for comparisons between multiple groups. The two-sample independent *t* test was used for

paired-group comparisons. *P* < 0.05 was considered statistically significant.

3. RESULTS

3.1. Identification of Core DEGs for T2DM. Differential gene analysis was conducted using three T2DM data sets from the GEO database. In cohort A, 4944 genes showed significant differences between normal and disease samples (adj-*p*-value < 0.01, \log_2 FCI > 1), with 2787 genes downregulated and 2157 genes upregulated (Figure 2A). Cohort B comprised 29 samples, with 174 DEGs between normal and disease groups (adj-*p*-value < 0.01, \log_2 FCI > 1), consisting of 27 downregulated and 147 upregulated genes (Figure 2B). Cohort C comprised 110 DEGs (adj-*p*-value < 0.05, \log_2 FCI > 1), comprising 56 downregulated and 54 upregulated genes (Figure 2C). Differentially expressed genes from cohorts A, B, and C were intersected using the “VennDiagram” package, resulting in a total of 15 common DEGs: CCR1, ACP5, NPL, CNTN4, NEXN, CHI3L1, CNN1, AQP9, IGHM, RGS1, CASQ2, MYOCD, MMRN1, CD163, and HMOX1 (Figure 2D). The STRING database was then used to construct a PPI network. Genes with mutual connections were retained, including CHI3L1, CD163, CCR1, AQP9, HMOX1, CNN1, MYOCD, CASQ2, and NEXN. PPI network analysis (Figure 2E) revealed nine nodes and seven edges, with 1.556 average neighbors, a network diameter of 3, a network radius of 1, a characteristic path length of 1.578, network density of 0.097, and 2 connected components.

3.2. mRNA Expression of Core DEGs between T2DM and Normal Tissues. Transcription expression levels were compared to validate the differences between normal and T2DM for the nine core DEGs. The results revealed significant differences in all nine core DEGs (*p* < 0.001). AQP9, CCR1, CD163, and CHI3L1 exhibited higher expression in T2DM compared to normal tissues, whereas CASQ2, CNN1, HMOX1, MYOCD, and NEXN exhibited lower expression in T2DM (Figure 3A–I).

3.3. Enrichment Analysis of Core DEGs. An enrichment analysis was performed on each gene to investigate the potential mechanisms of these nine genes. The enrichment results (Figure 4A–I) indicate that these genes are enriched in biological functions related to leukocyte migration and adaptive immune response. Most genes were enriched in biological functions related to leukocyte chemotaxis, bone marrow cell–mediated immunity, bone marrow cell migration, and positive regulation of activated cell functions. A few genes were enriched in other biological functions, such as CNN1 in single-cell migration, CASQ2 in regulating activated cells and I BAND, and AQP9 in neutrophil migration. Moreover, regarding cellular pathways influenced by these genes, all genes are enriched in lysosome and hematopoietic cell lineage regulation pathways. The major signaling pathways include B-cell receptor signaling, Toll-like receptor signaling, cytokine receptor interaction, and natural killer cell–mediated cytotoxicity (Figure 4A–I and Table 2).

GO and KEGG enrichment analyses indicated that the core genes are enriched to varying degrees in functions related to vascular smooth muscle, sarcomere, sarcoplasmic reticulum membrane, and phosphoric diester hydrolase activity (Figure 4J). These core genes are also enriched in pathways related to ferroptosis, porphyrin metabolism, mineral absorption, cardiac muscle contraction, and other related pathways (Figure 4J). Additionally, the Metascape enrichment analysis (Figure 5A,B)

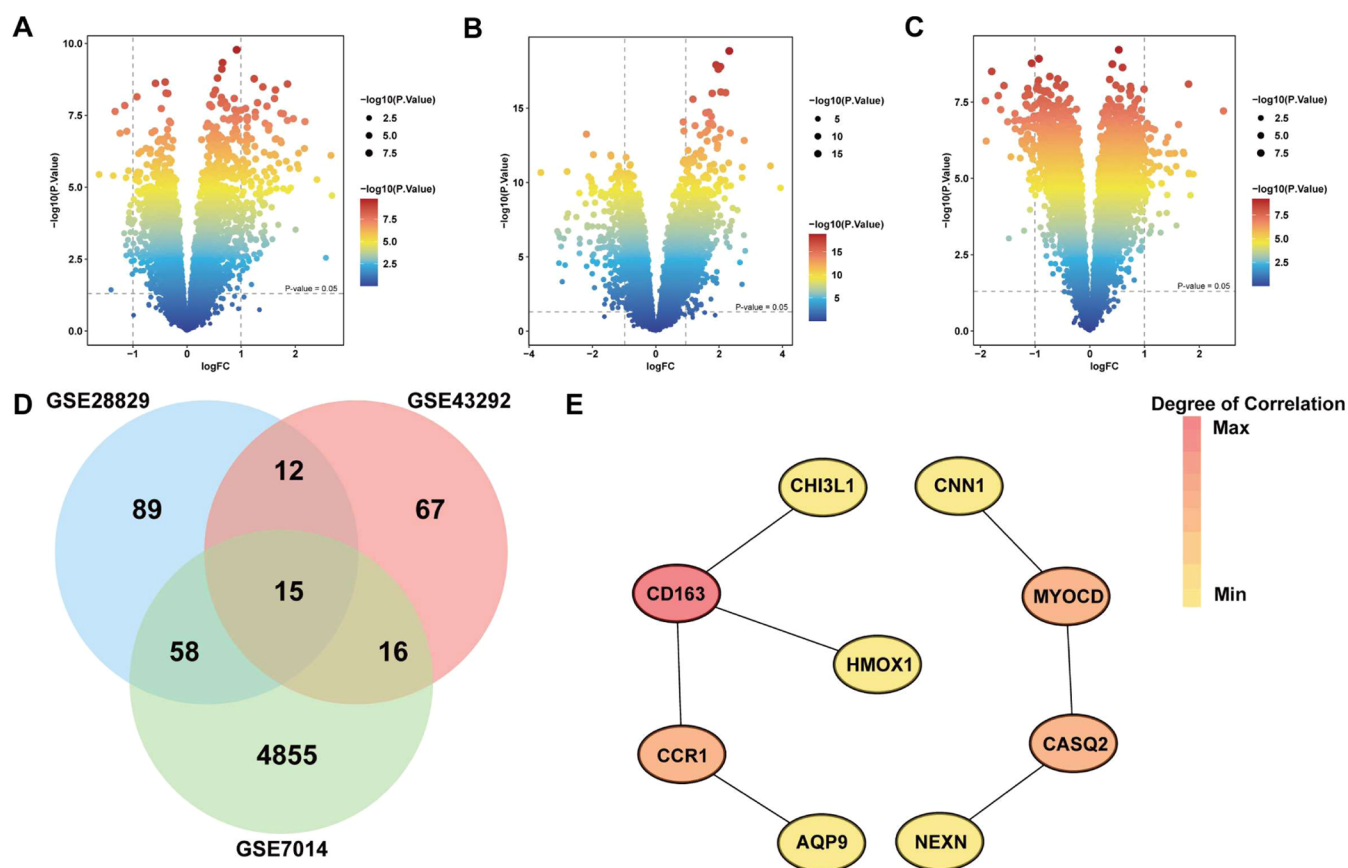


Figure 2. DEGs screen. Volcano plots of the DEGs in (A) GSE7014, (B) GSE28829, and (C) GSE43292 (Significance increases from blue to red, with deeper red indicating higher significance of DEGs. The two vertical dashed lines denote $|\log FC| = 1$, and the horizontal dashed line indicates $P\text{-value} = 0.05$). (D) Shared DEGs. (E) Protein–protein interaction network of the top nine core DEGs.

showed that the core genes play a significant role in the negative regulation of smooth muscle cell proliferation, inflammatory responses, and maintaining cellular monovalent inorganic cation homeostasis.

3.4. Constructing the Risk Prediction Model and Validation. Risk prediction models were constructed to explore the accuracy of core genes in predicting the risk of T2DM. By assessing the diagnostic effectiveness of T2DM, ROC curves are calculated individually for the core genes, including CD163, CCR1, MYOCD, CASQ2, CNN1, CHI3L1, HMOX1, NEXN, and AQP9. The results indicate AUC values of 0.714, 0.794, 0.843, 0.738, 0.865, 0.671, 0.737, 0.751, and 0.700 (Figure 5C), respectively, affirming the reliability of the genes selected for T2DM. A nomogram of the model was also used to predict the risk of T2DM. Low expression of CASQ2, MYOCD, HMOX1, CNN1, and NEXN may promote disease onset. In contrast, low expression of CD163, CHI3L1, CCR1, and AQP9 has an inhibitory effect on disease onset (Figure 5E). Overall, the predicted risk of T2DM aligns well with the calibration plot (Figure 5D,E), reflecting the strong reliability of the model.

3.5. Immune Infiltration Analysis. To investigate the relationship between the expression of core genes in T2DM and various immune cell types, we analyzed differential gene expression in 22 distinct immune cell populations. The samples were categorized into experimental and control groups, allowing for a comparative assessment of immune cell infiltration between high-risk and low-risk cohorts. This analysis facilitated the elucidation of correlations among the

immune cell types. The results (Figure 6A) reveal a negative correlation between the expression levels of T cells CD4 memory activated and several immune cells, including macrophages M1, dendritic cells resting, mast cells activated, and B cell memory. Conversely, a positive correlation was observed between mast cells resting and B cell memory, as well as plasma cells. Furthermore, a comparison of immune cell infiltration between the experimental and control groups highlighted statistically significant differences in the populations of T cells CD8 ($p < 0.001$), T cells γ delta ($p = 0.048$), NK cells activated ($p = 0.001$), monocytes ($p = 0.002$), macrophages M0 ($p < 0.001$), macrophages M1 ($p = 0.013$), and dendritic cells resting ($p = 0.031$), thereby underscoring the robust association between these seven immune cell types and the therapeutic management of T2DM (Figure 6B).

HMOX1 was subsequently selected as a representative marker to further investigate its correlation with various immune-infiltrating cells in T2DM. The results indicate a relationship between HMOX1 expression and eight different types of immune-infiltrating cells (Figure 6C–K). Specifically, HMOX1 shows a positive correlation with macrophages M0 ($r = 0.65$, $p < 0.001$) and T cells γ delta ($r = 0.36$, $p = 0.0029$). Conversely, HMOX1 displays a negative correlation with NK cells activated ($r = -0.28$, $p = 0.021$), T cells CD4 memory resting ($r = -0.35$, $p = 0.0037$), monocytes ($r = -0.36$, $p = 0.0023$), B cells naive ($r = -0.43$, $p < 0.001$), dendritic cells activated ($r = -0.45$, $p < 0.001$), and T cells CD8 ($r = -0.52$, $p < 0.001$).

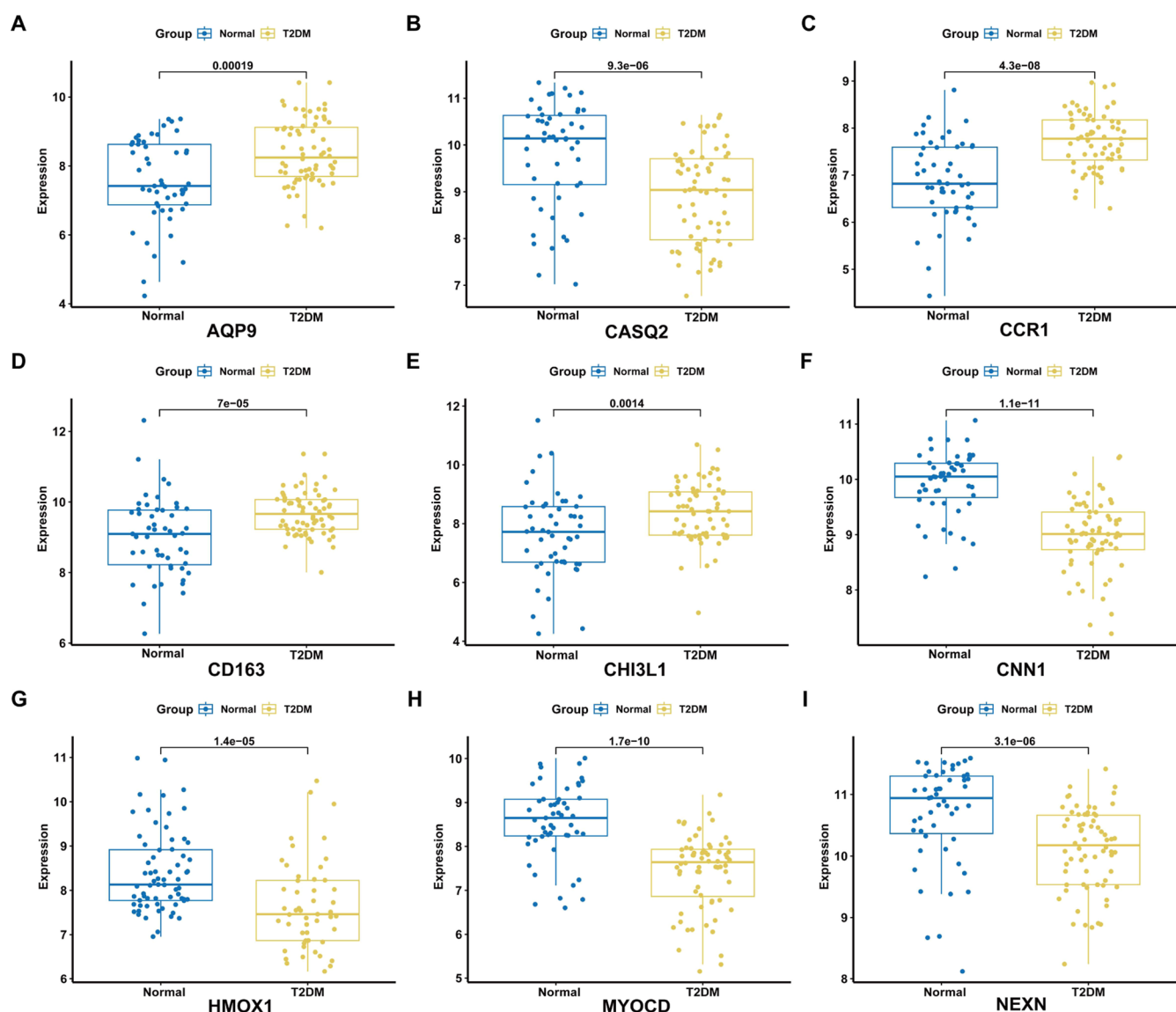


Figure 3. Transcript expression of core DEGs. (A) AQP9, (B) CASQ2, (C) CCR1, (D) CD163, (E) CHI3L1, (F) CNN1, (G) HMOX1, (H) MYOCD, and (I) NEXN in normal and T2DM data sets.

3.6. Experimental Verification. Compared to the db/m group, db/db mice displayed typical diabetic symptoms, including increased body weight and elevated FBG levels (Figure 7A–C). Over the course of 12 weeks of feeding, db/db mice consistently exhibited higher body weight and FBG levels compared to their db/m counterparts during the same period ($P < 0.001$). Notably, while the body weight of db/db mice showed a gradual decline, FBG levels continuously rose, with a statistically significant difference observed compared to the beginning of the feeding period ($P < 0.05$). HbA1c, FINS, and HOMA-IR levels were higher in db/db mice than in db/m mice ($P < 0.001$) (Figure 7D–F). Additionally, db/db mice demonstrated pronounced hepatic steatosis and elevated lipid levels compared to the db/m group, as indicated by increases in TC, triglycerides (TG), and LDL-C, alongside a decrease in HDL-C levels (Figure 7G–J). H&E staining of liver tissue revealed substantial hepatocellular vacuolation and the presence of lipid droplets in db/db mice, whereas the liver tissue of db/m mice appeared more intact with fewer vacuoles and lipid droplets (Figure 7K,L).

To evaluate the differential expression of HMOX1 in T2DM, we examined the serum levels of HMOX1 in mice from the db/db and db/m groups. Serum HMOX1 was significantly lower in the db/db group than in normal mice ($P < 0.01$), consistent with the difference analysis (Figures 3G and 8A). Additionally, we assessed the expression of HMOX1 protein and mRNA in the liver using Western blotting and qPCR. The results showed that the liver HMOX1 content was significantly lower in diabetic mice than in the controls (Figure 8B–D). Furthermore, the expression of NFE2L2, an upstream regulator of HMOX1, was analyzed. The results demonstrated that both protein and mRNA levels of NFE2L2 were significantly higher in the normal group than in the diabetic group (Figure 8B–D). Immunohistochemical analysis revealed pathological alterations in the liver that were consistent with the H&E staining, thereby supporting the earlier conclusions (Figure 8E,F).

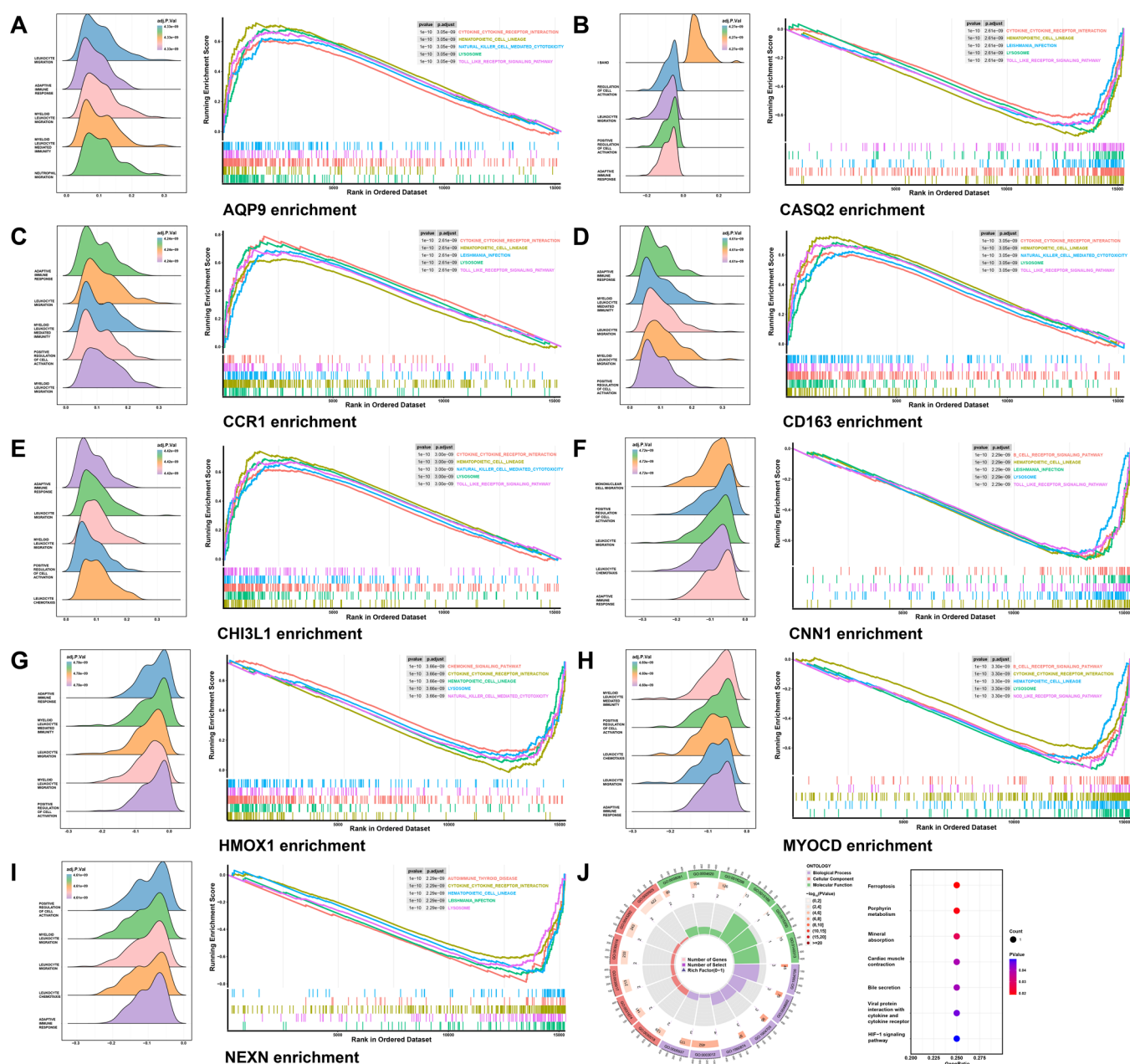


Figure 4. Biological function and relationship of nine core DEGs. (A–I) The top five most enriched functions and pathways in CD163, CCR1, MYOCD, CASQ2, CNN1, CHI3L1, HMOX1, NEXN, and AQP9. (J) The biological function (left) and pathway (right) of nine core DEGs.

4. DISCUSSION

T2DM is a complex and chronic condition characterized by elevated blood glucose levels, resulting from either a relative or absolute deficiency of insulin due to pancreatic β -cell dysfunction.²⁶ According to the International Diabetes Federation, the global prevalence of diabetes among adults aged 20–79 years reached 10.2% in 2021 and is projected to rise to 12.2% by 2045, affecting up to 783.2 million individuals.²⁷ China has emerged as one of the countries experiencing the fastest increase in diabetes prevalence worldwide.²⁸ As the duration of diabetes extends, persistent hyperglycemia can lead to irreversible damage to nerves, blood vessels (both microvascular and macrovascular), and various organs. The emergence of numerous complications has a significant impact on patients' quality of life and can even pose life-threatening risks.²⁹ Thus, gaining a deeper understanding

of biomarkers that can predict the onset and progression of diabetes is crucial for early intervention and for potentially reversing or delaying the disease's advancement.

In this study, we aimed to identify potential predictive biomarkers for T2DM by analyzing significant DEGs found in three distinct data sets from the GEO database. Ultimately, we retained nine DEGs that exhibited mutual associations: CHI3L1, CD163, CCR1, AQP9, HMOX1, CNN1, MYOCD, CASQ2, and NEXN. These genes demonstrated significant differences between healthy individuals and those with T2DM (Figure 3A–I). Upon examining the biological processes associated with these core genes, we discovered that they were enriched in functions related to leukocyte migration and the adaptive immune response (Figure 4A–I). Patients with T2DM exhibit a chronic activation of the islet innate immune system, characterized by heightened local and systemic

Table 2. Main Functions and Pathways of Core DEGs

serial number	core DEGs	functions	pathways	serial number	core DEGs	functions	pathways
1	AQP9	leukocyte migration	hematopoietic cell lineage			myeloid leukocyte migration	cytokine cytokine receptor interaction
		adaptive immune response	natural killer cell mediated cytotoxicity			positive regulation of cell activation	lysosome
		myeloid leukocyte migration	cytokine cytokine receptor interaction			leukocyte chemotaxis	toll like receptor signaling pathway
		myeloid leukocyte mediated immunity	lysosome	6	CNN1	mononuclear cell migration	B cell receptor signaling pathway
		neutrophil migration	toll like receptor signaling pathway			positive regulation of cell activation	hematopoietic cell lineage
2	CASQ2	I band	cytokine cytokine receptor interaction			leukocyte migration	Leishmania infection
		regulation of cell activation	Leishmania infection			leukocyte chemotaxis	lysosome
		leukocyte migration	hematopoietic cell lineage			adaptive immune response	toll like receptor signaling pathway
		positive regulation of cell activation	lysosome	7	HMOX1	adaptive immune response	chemokine signaling pathway
		adaptive immune response	toll like receptor signaling pathway			myeloid leukocyte mediated immunity	cytokine cytokine receptor interaction
3	CCR1	adaptive immune response	cytokine cytokine receptor interaction			leukocyte migration	hematopoietic cell lineage
		leukocyte migration	hematopoietic cell lineage			myeloid leukocyte migration	lysosome
		myeloid leukocyte mediated immunity	Leishmania infection			positive regulation of cell activation	natural killer cell mediated cytotoxicity
		positive regulation of cell activation	lysosome	8	MYCOD	myeloid leukocyte mediated immunity	B cell receptor signaling pathway
		myeloid leukocyte migration	toll like receptor signaling pathway			positive regulation of cell activation	cytokine cytokine receptor interaction
4	CD163	adaptive immune response	hematopoietic cell lineage			leukocyte chemotaxis	hematopoietic cell lineage
		myeloid leukocyte mediated immunity	natural killer cell mediated cytotoxicity			leukocyte migration	lysosome
		leukocyte migration	cytokine cytokine receptor interaction			adaptive immune response	nod like receptor signaling pathway
		myeloid leukocyte migration	lysosome	9	NEXN	positive regulation of cell activation	autoimmune thyroid disease
		positive regulation of cell activation	toll like receptor signaling pathway			myeloid leukocyte migration	cytokine cytokine receptor interaction
5	CHI3L1	adaptive immune response	hematopoietic cell lineage			leukocyte migration	hematopoietic cell lineage
		leukocyte migration	natural killer cell mediated cytotoxicity			leukocyte chemotaxis	Leishmania infection
						adaptive immune response	lysosome

cytokine production, along with increased local infiltration of immune cells—these factors play a pivotal role in the pathogenesis of the disease.^{30,31}

Numerous studies have shown that the increased presence and activation of both innate and adaptive immune cells in adipose tissue contribute to the enhanced release of local and systemic inflammatory cytokines and chemokines. This low-grade, chronic inflammation, induced by leukocytes, is responsible for impairments in insulin signaling across adipose tissue, the liver, and skeletal muscle.^{32,33} Consequently, this leads to IR and elevated blood glucose levels, which are primary contributors to T2DM.

Furthermore, in patients with T2DM, islet inflammation is often accompanied by amyloid deposition, fibrosis, macrophage infiltration, and an increased expression of proinflammatory cytokines and chemokines. These changes ultimately cause disruptions in insulin secretion and induce β cell apoptosis, culminating in the development of T2DM.³⁴ Monocyte infiltration is also recognized as a major risk factor for the development of long-term diabetic complications such

as neuropathy, retinopathy, nephropathy, and other microvascular diseases.³⁵ Given these findings, we propose that the regulation of chronic low-grade inflammation in T2DM may represent a critical underlying mechanism associated with the function of the nine identified genes.

The infiltration of a diverse array of immune cells, including macrophages, T lymphocytes, B lymphocytes, and natural killer cells, into visceral tissues, alongside the ongoing activation of immune responses and metabolic dysregulation, is a prominent feature in the pathogenesis of T2DM.^{36,37} In subsequent investigations, we examined the relationship between key genes and the infiltration of immune cells. Our findings demonstrated that the expression variations of nine core genes significantly influenced several immune cell types, including CD8+ T cells, γ delta T cells, activated NK cells, monocytes, M0 and M1 macrophages, and resting dendritic cells. Notable differences were observed between the experimental and control groups, suggesting a close association with T2DM treatment (Figure 6A,B).

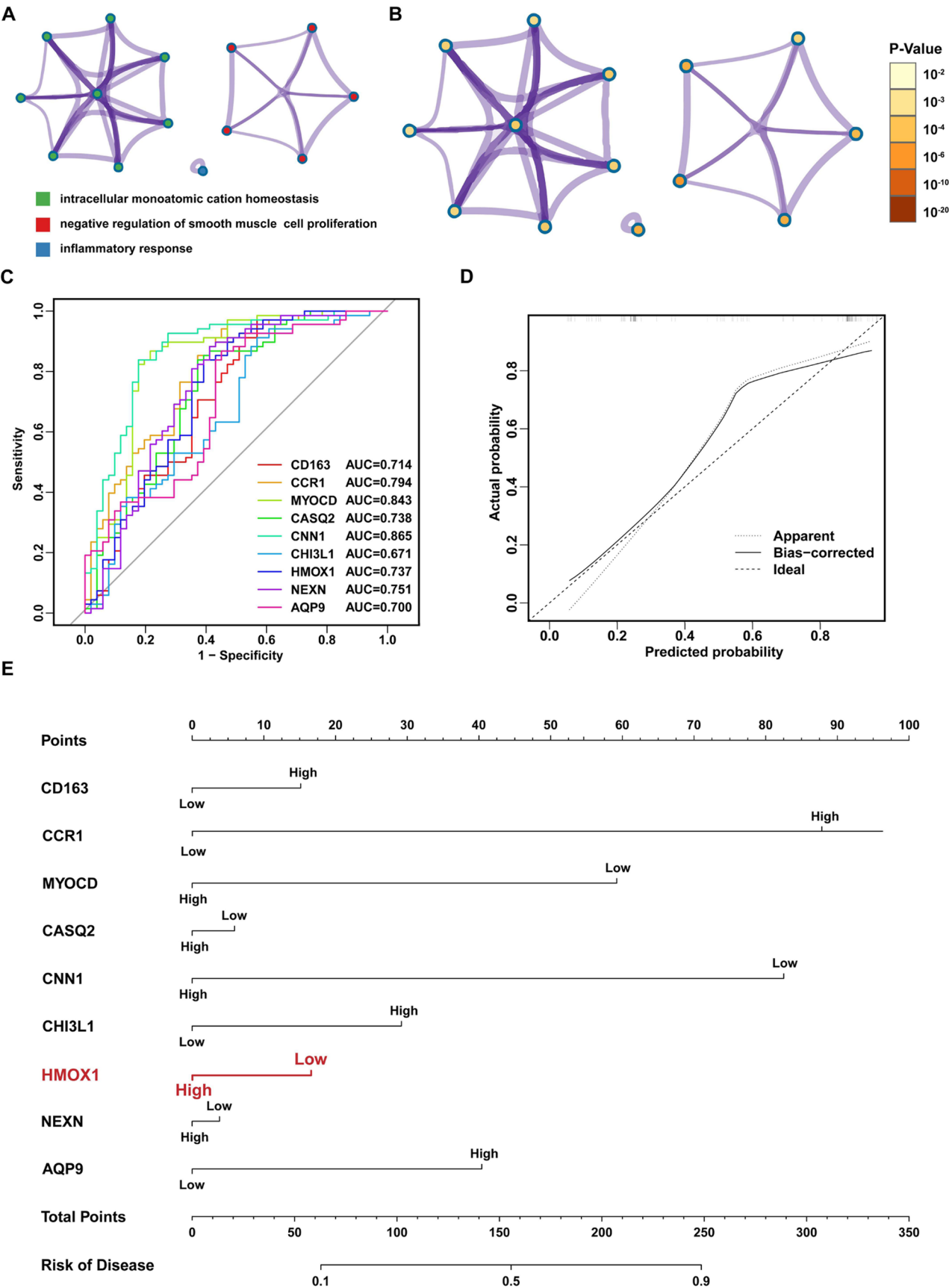


Figure 5. Nine core DEGs expression and function profiles and an evaluation of the prediction model in T2DM. (A) Pathway enrichment. (B) The degree of enrichment. (C) Predictive accuracy of the model. (D) Calibration curve based on the prediction model. (E) Risk score of the prediction model.

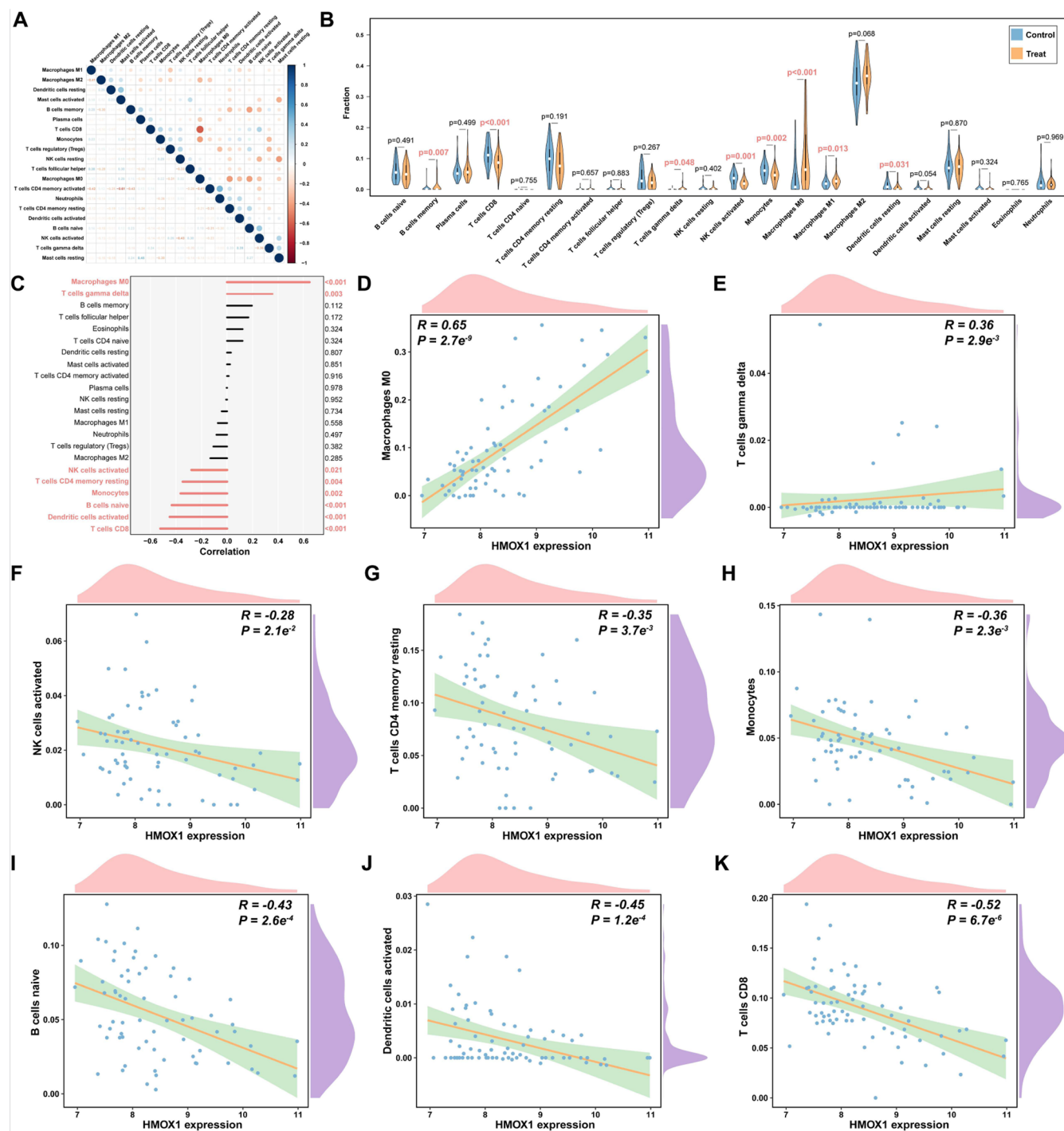


Figure 6. Expression of core DEGs and HMOX1 with immune infiltration in the T2DM microenvironment. (A) Comparison of 22 immune cell types in T2DM. (B) Comparison of core DEGs between high and low-expression groups in 22 immune cell types. (C–K) Correlation between HMOX1 and immune cell expression in T2DM. Macrophages M0, T cells γ delta, NK cells activated, T cells CD4 memory resting, monocytes, B cells naive, dendritic cells activated, T cells CD8. (T cells: T lymphocyte, B cells: B lymphocyte, NK cells: natural killer cells, Macrophages M1: classically activated macrophages, Neutrophils: polymorphonuclear neutrophils).

Further exploration of the correlation between HMOX1 and immune cell infiltration reinforced the observation that HMOX1 exhibited significant correlations with eight immune cell types, including M0 macrophages, γ delta T cells, activated NK cells, resting memory CD4+ T cells, monocytes, naive B cells, and activated dendritic cells (Figure 6C–K). Macrophages, being the predominant innate immune cells within adipose tissue, play a pivotal role in the metabolic

inflammation associated with T2DM. M0 macrophages are instrumental in the phagocytosis and clearance of cellular debris, marking the initiation of the inflammatory response. In contrast, M1 macrophages function as immunostimulatory entities, producing extensive quantities of inflammatory mediators, thus serving as a primary source of proinflammatory cytokines and chemokines within the organism.^{36,37} In the context of obesity and IR, macrophages undergo proliferation

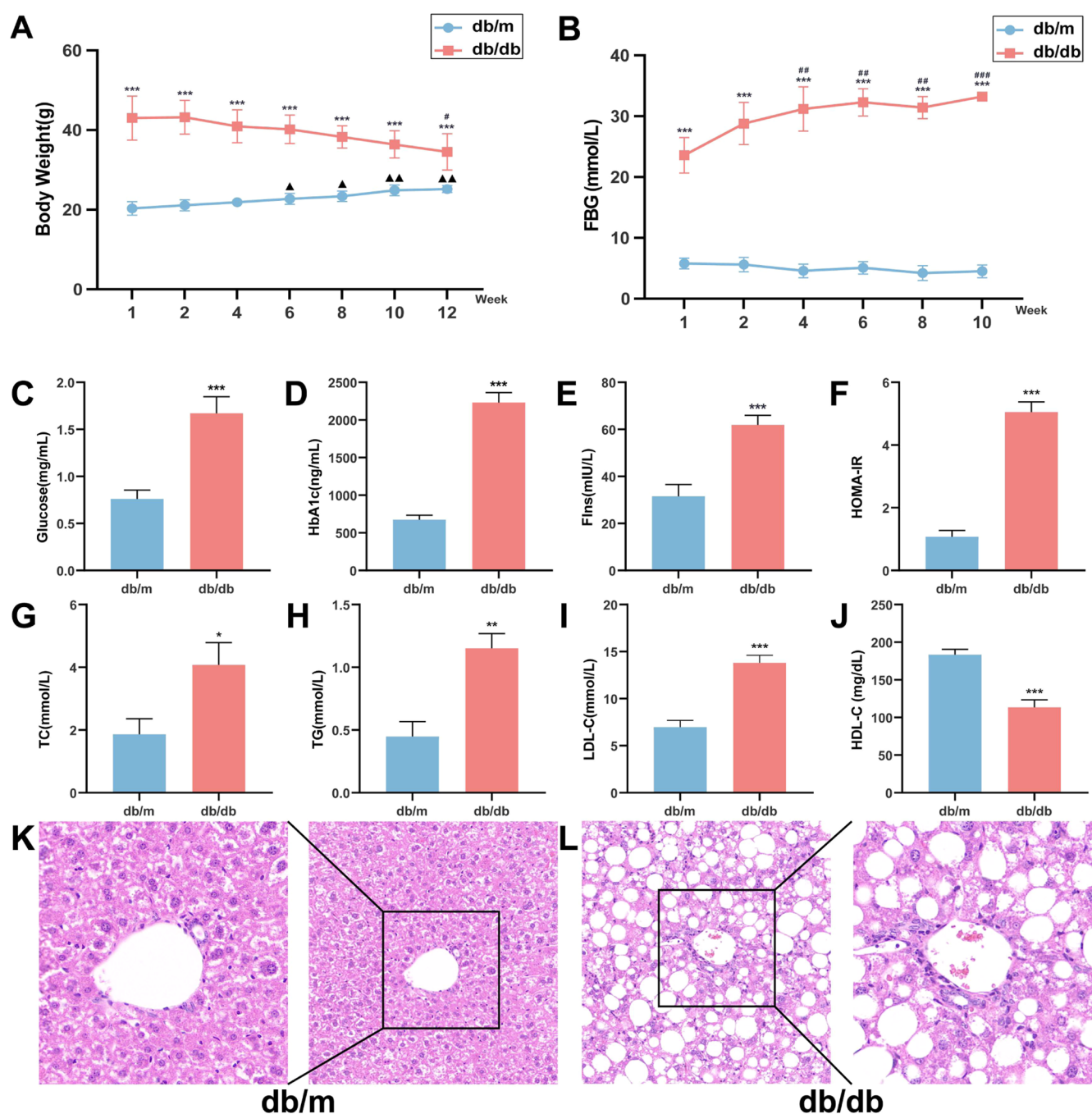


Figure 7. Characterization of the db/m and db/db mice. (A and B) Body weight and Fasting blood glucose. (C–F) Blood chemistry indicators of glucose and insulin function. (G–J) Lipid levels. (K and L) H&E-stained liver samples. Compared with the same group at 1 week, # $p < 0.05$, ## $p < 0.01$, ### $p < 0.001$, ▲ $p < 0.05$, ▲▲ $p < 0.01$. Compared with the db/m group, * $p < 0.05$; ** $p < 0.01$; *** $p < 0.001$.

and accumulate in visceral tissues, leading to a significant polarization toward M1 macrophages as proinflammatory monocytes migrate and differentiate within adipose tissues. This phenomenon results in an imbalance in the M1/M2 macrophage ratio.³⁸ The persistent elevation of proinflammatory factors adversely impacts glucose metabolism and the reparative processes in visceral tissues, culminating in insulin dysfunction and potential dysfunction or apoptosis of pancreatic islet β cells.³⁹ These mechanisms are critical in the onset and progression of T2DM, corroborating our findings that both M0 and M1 macrophages exhibit heightened expression levels in T2DM (Figure 6B).

HMOX1 plays a critical role in the regulation of macrophage polarization, facilitating the transition from the M1 proinflammatory state to the M2 anti-inflammatory state.²¹ In patients with T2DM, there is a noted increase in M1 macrophage polarization and the expression of proinflammatory cytokines, concomitant with a decrease in M2 macrophage polarization and anti-inflammatory cytokine expression. Activation of HMOX1 inhibits macrophage-to-M1 polarization, significantly reduces the expression of proinflammatory cytokines interleukin IL-6, IL-1 β , and inducible nitric oxide synthase, and increases the expression of anti-inflammatory factor IL-10.⁴⁰ Notably, M2 macrophage polarization appears

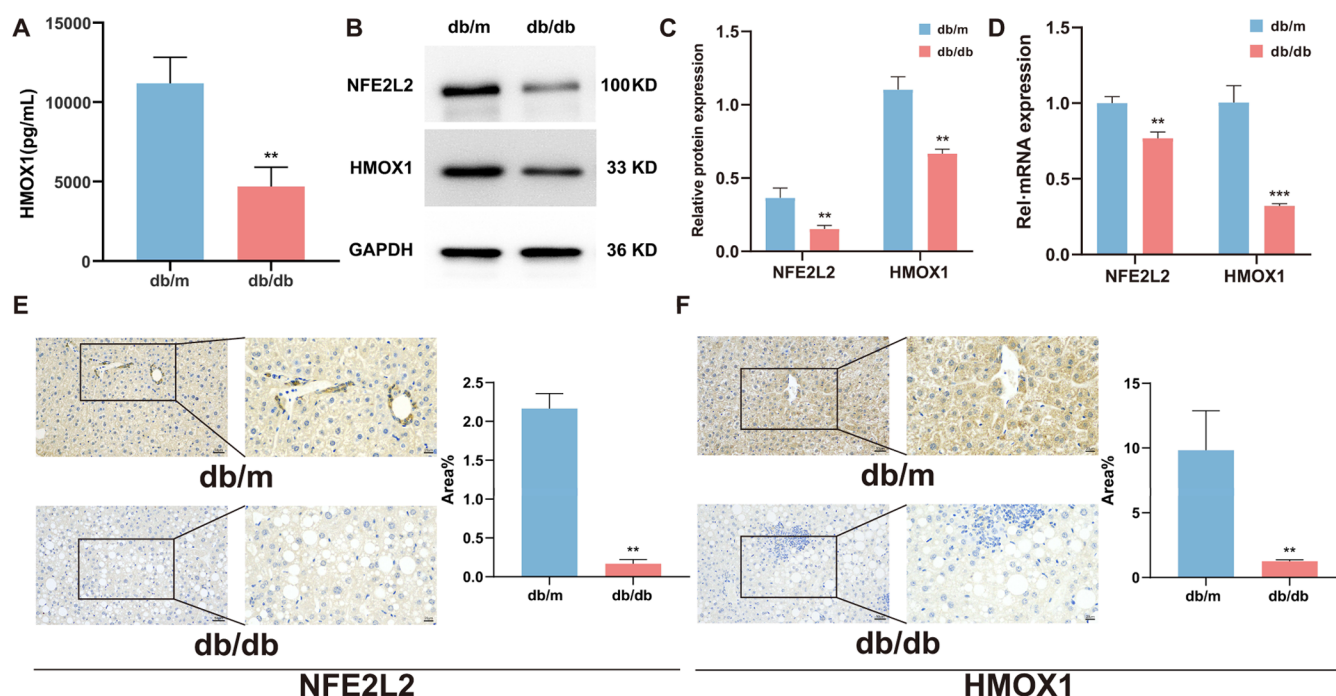


Figure 8. Comprehensive analysis of NFE2L2 and HMOX1 in db/m and db/db mice. (A) Serum HMOX1 levels. (B and C) Western blot analysis of NFE2L2 and HMOX1. (D) Transcript expression of NFE2L2 and HMOX1. Immunohistochemical analysis of (E) NFE2L2 and (F) HMOX1. Compared with the db/m group, * $p < 0.05$; ** $p < 0.01$; *** $p < 0.001$.

to be positively correlated with HMOX1 expression in the context of diabetes. Short-term induction of HMOX1 has been shown to foster a protective M2-like microenvironment within the pancreas, thereby exhibiting immunomodulatory and prorepair effects relevant to diabetic pathology.⁴¹ While investigations into the interplay between HMOX1 and macrophages in diabetes and its complications remain limited, the capacity of macrophages to maintain microenvironmental stability, along with the antioxidant and anti-inflammatory properties attributed to HMOX1, suggest that targeting HMOX1 in conjunction with macrophage modulation may represent a viable therapeutic strategy for managing diabetes.

The results of the current study indicate that the TLR signaling pathway is a significant mechanism through which the nine core genes operate (Figure 4A–I). The TLR family serves as one of the initial responders within the immune system. Acting as a crucial intermediary between specific and nonspecific immunity, it plays a vital role in activating inflammatory processes and is regarded as a contributor to the development of chronic diseases, including obesity, T2DM, and cardiovascular disease.³⁰ Previous research has demonstrated that the mRNA expression levels of TLR2 and TLR4 in the peripheral blood monocytes of T2DM patients are elevated, facilitating the activation of the FFA-induced inflammatory pathway and metabolic signaling in IR via the NF- κ B pathway.^{42,43} The TLR4 pathway may induce the autophosphorylation of insulin receptor substrates or engage in hypothalamic inflammation, which disrupts the insulin signaling cascade, blocks substrate binding to the insulin receptor, and ultimately results in IR.⁴⁴ Accumulating evidence has demonstrated the regulatory role of HMOX1 in the TLR signaling pathway, including its negative feedback inhibition of TLR4-dependent MyD88-NF- κ B activation, suppression of pro-inflammatory cytokine expression (TNF- α , IL-6, IL-1 β),⁴⁵ and interference with the TLR4-dependent TRIF pathway. By

inhibiting the phosphorylation of TRAF6 and TAK1, HMOX1 can reduce the expression of IRF3, thereby mitigating chronic inflammation induced by TLR4 activation.⁴⁶ Furthermore, the anti-inflammatory effects of HMOX1 have been demonstrated in pancreatic inflammation induced in vitro, wherein TLR4 expression in pancreatic islets is downregulated by HMOX1 agonists, leading to the suppression of COX-2, CCL-2, IL-6, and ROS, thereby exerting anti-inflammatory and antioxidant effects.⁴⁷ Given the important role of the TLR pathway in T2DM and its close association with HMOX1, it is hypothesized that the interconnection between the predicted genes and the TLR pathway could offer valuable insights into the pathogenesis and potential therapeutic strategies for T2DM.

The results from the Metascape analysis demonstrated that these core genes significantly influence the function of vascular smooth muscle cells (VSMCs) (Figure 5A,B). The abnormal proliferation and migration of VSMCs are critical factors in vascular intimal changes. Persistent hyperglycemia, commonly associated with diabetes, has been shown to induce premature senescence in both endothelial cells and VSMCs, accelerating endothelial dysfunction in both microvessels and macrovasculature. This process leads to arterial wall thickening, alterations in the collagen and elastin components of the extracellular matrix, arteriosclerosis, and various other structural and functional changes, ultimately contributing to the development of vascular complications in T2DM.^{48,49} The emergence of macrovascular and microvascular complications of diabetes—including atherosclerosis, cardiomyopathy, nephropathy, and retinopathy—represents a primary concern affecting the quality of life and work of patients in the later stages of the disease and can even pose a threat to their lives.^{50,51} Therefore, we propose that the nine core genes identified not only serve as valuable predictors for the onset of T2DM but also hold significant predictive and therapeutic

potential regarding the vascular complications triggered by hyperglycemia as the disease progresses.

A risk prediction model for T2DM was developed, confirming the reliability of the nine core genes identified for predicting the onset of the disease (Figure 5C). The nomogram results revealed that elevated expression levels of AQP9, CCR1, CD163, and CHI3L1 contribute to the onset of T2DM, whereas higher expression of CNN1, CASQ2, HMOX1, MYOCD, and NEXN appears to inhibit its development (Figure 5E).

As an integral component of the antioxidant response element, HMOX1 binds to crucial factors, such as NFE2L2, within the endogenous cellular defense mechanism in response to oxidative stress. This pathway plays a significant role in the restoration of intracellular homeostasis. The activation of the NFE2L2/HMOX1 pathway has been demonstrated to mitigate oxidative stress and apoptosis, particularly in the context of diabetes.^{52,53} In comparative analyses, db/db mice exhibited typical diabetic phenotypes, including hyperglycemia, hyperlipidemia, and IR, alongside pathological evidence of pronounced hepatic steatosis (Figure 7). This study assessed the expression levels of NFE2L2 and HMOX1 in the serum and liver of both db/m and db/db groups. Notably, the findings revealed a significant reduction in HMOX1 expression in the serum and liver of db/db mice, accompanied by decreased protein and mRNA levels of NFE2L2 in the T2DM group (Figure 8). These experimental results provide further confirmation of the diminished expression of HMOX1 in T2DM.

Given the genetic and physiological similarities between mice and humans, along with the homologous nature of HMOX1 in both species, there exists substantial potential for the applicability of these findings to human populations. However, it is imperative to acknowledge that while HMOX1 has demonstrated promise as a biomarker in animal models, there may be unrecognized or uncontrolled confounding variables that could impact the accuracy and reliability of HMOX1 as a biomarker in clinical settings. Consequently, further clinical investigations are warranted to validate the relevance and validity of HMOX1 in human diabetes. Future studies are being planned to gather additional clinical samples, including blood from T2DM patients, to further elucidate the key findings of this study, specifically focusing on the expression level, the functionality of HMOX1, and its correlation with other biomarkers.

In summary, our research started initiated with the mining of the GEO database, ultimately identifying nine core DEGs through computational algorithms. GO and KEGG analyses verified that the effects of these core genes on T2DM are primarily associated with inflammation and immune responses, wherein their respective action pathways were notably enriched. A risk prediction model was subsequently constructed to assess the predictive reliability of these core genes regarding the onset of T2DM, along with an evaluation of the relationship between the core DEGs and immune cell infiltration. Notably, HMOX1 emerged as a representative gene, warranting further investigation into its correlation with 22 immune cell types. Our findings substantiate the relationship between HMOX1 and T2DM and reveal a significant downregulation of HMOX1 expression in T2DM, as substantiated by animal model experiments. Consequently, we postulate that HMOX1 may serve as a novel and promising target for both the prediction and therapeutic intervention of

T2DM, potentially influencing the persistent chronic low-grade inflammation and adaptive immune responses characteristic of this condition.

The specific mechanisms underlying this relationship merit further extensive investigation and may be related to oxidative stress responses mediated by NFE2L2. Furthermore, the remaining eight genes explored in this study may similarly partake in the onset and progression of T2DM. We anticipate that the methodologies employed to elucidate the relevance of HMOX1 in this study can be translated to other genetic candidates, thereby facilitating the identification of additional biomarkers with prognostic significance for T2DM.

It is worth noting that the screening and analysis of differential genes in this investigation were conducted based on pre-existing data sets. Although thorough screening and analysis were performed, the statistical power and generalizability of the findings may be compromised by the limited sample size and inherent constraints of the data sets. Moreover, the considerable differences between experimental animal models and human T2DM must be acknowledged, as the pathophysiological complexity of human T2DM cannot be fully recapitulated by findings from db/db mice alone. Therefore, further basic and clinical studies are necessary to further validate the findings and explore potential molecular mechanisms.

5. CONCLUSION-S

The prevalence of diabetes has significantly increased worldwide, presenting a considerable challenge to public health management and healthcare costs worldwide. The ongoing development of diabetes is frequently associated with various comorbidities and complications. Internationally, prevention and management strategies for diabetes and its associated complications are crucial. In addition to several well-established interventions recognized globally, such as diet modifications, lifestyle changes, medications, and even metabolic surgery, there is growing emphasis on the importance of timely interventions.⁵⁴ Early intervention for individuals who are newly diagnosed or in a prediabetic state can yield the most effective results. As a result, exploring biomarkers that can effectively warn of or facilitate treatment for T2DM in its early stages is of great significance.

Mining public databases represents an effective, feasible, and cost-efficient approach to discovering potential disease biomarkers. Research has indicated that the expression of HMOX1 is significantly reduced in diabetic mice exhibiting glucose and lipid metabolism disorders, suggesting it could serve as a novel biomarker for T2DM. Furthermore, the strong association of HMOX1 with immune cells, particularly macrophages, alongside its link to NFE2L2, highlights its excellent antioxidant and anti-inflammatory properties. These attributes promise to enhance the potential of HMOX1 activators as a viable treatment for T2DM and related inflammatory diseases. However, these findings necessitate further evaluation for their validity and accuracy through clinical trials.

■ AUTHOR INFORMATION

Corresponding Authors

Jindong Zhao – The First Affiliated Hospital, Anhui University of Chinese Medicine, Hefei, Anhui 230038, China; School of Chinese Medicine, Anhui University of Chinese

Medicine, Hefei, Anhui 230012, China;

Email: zhaojindong1111@163.com

Zhaohui Fang – The First Affiliated Hospital, Anhui

University of Chinese Medicine, Hefei, Anhui 230038, China;

Email: fangzhaohui1111@163.com

Authors

Qi Xu – The First Affiliated Hospital, Anhui University of Chinese Medicine, Hefei, Anhui 230038, China; School of Chinese Medicine, Anhui University of Chinese Medicine, Hefei, Anhui 230012, China; orcid.org/0009-0001-4881-3049

Hongrong Zhang – School of Medical Informatics Engineering, Anhui University of Chinese Medicine, Hefei, Anhui 230012, China

Nuobing Ruan – The First Affiliated Hospital, Anhui University of Chinese Medicine, Hefei, Anhui 230038, China

Jiawen Jing – The First Affiliated Hospital, Anhui University of Chinese Medicine, Hefei, Anhui 230038, China

Yufan Li – The First Affiliated Hospital, Anhui University of Chinese Medicine, Hefei, Anhui 230038, China

Complete contact information is available at:

<https://pubs.acs.org/10.1021/acsomega.4c09662>

Author Contributions

[†]H.R.Z. and N.B.R. contributed equally to this study and should be considered as cofirst authors. Conceptualization and design of the research: Z.H.F. and J.D.Z. Methodology: H.R.Z. and N.B.R. Acquisition and analysis of data: H.R.Z., J.W.J., and Y.F.L. Software: H.R.Z. and Q.X. Visualization of data: H.R.Z., Q.X., and N.B.R. Validation: Q.X., N.B.R., and Y.F.L. Writing—original draft preparation: Q.X. and H.R.Z. Writing—review and editing: Q.X. and N.B.R. Project administration: J.D.Z. Supervision: J.D.Z. and Z.H.F. Funding acquisition: Z.H.F. All authors have read and agreed to the published version of the manuscript.

Funding

This study is supported by the National Natural Science Foundation of China (82174153), the Collaborative Innovation Project for Universities of Anhui Province (GXXT-2020-025), and the National Key R&D Program “Strategic International Science and Technology Innovation Cooperation” (2020YFE201800).

Notes

The authors declare no competing financial interest.

REFERENCES

- (1) Singh, D. D.; Shati, A. A.; Alfaifi, M. Y.; Elbehairi, S.; Han, I.; Choi, E. H.; Yadav, D. K. Development of dementia in type 2 diabetes patients: mechanisms of insulin resistance and antidiabetic drug development. *Cells* **2022**, *11* (23), No. 3767.
- (2) Sobiecki, J. G.; Imamura, F.; Davis, C. R.; Sharp, S. J.; Koulman, A.; Hodgson, J. M.; Guevara, M.; Schulze, M. B.; Zheng, J. S.; Agnoli, C.; et al. A nutritional biomarker score of the mediterranean diet and incident type 2 diabetes: integrated analysis of data from the medley randomised controlled trial and the epic-interact case-cohort study. *PLOS Med.* **2023**, *20* (4), No. e1004221.
- (3) Organization, W. H. *Global Report on Neglected Tropical Diseases 2023*, World Health Organization 2023.
- (4) Zhao, Y.; Li, Y.; Zhuang, Z.; Song, Z.; Wang, W.; Huang, N.; Dong, X.; Xiao, W.; Jia, J.; Liu, Z.; et al. Associations of polysocial risk score, lifestyle and genetic factors with incident type 2 diabetes: a prospective cohort study. *Diabetologia* **2022**, *65* (12), 2056–2065.
- (5) Arte, P. A.; Tungare, K.; Bhoori, M.; Jobby, R.; Aich, J. Treatment of type 2 diabetes mellitus with stem cells and antidiabetic drugs: a dualistic and future-focused approach. *Hum. Cell* **2024**, *37* (1), 54–84.
- (6) Chen, S.; Gan, D.; Lin, S.; Zhong, Y.; Chen, M.; Zou, X.; Shao, Z.; Xiao, G. Metformin in aging and aging-related diseases: clinical applications and relevant mechanisms. *Theranostics* **2022**, *12* (6), 2722–2740.
- (7) Ricci, M.; Mancebo-Sevilla, J. J.; Cobos, P. L.; Sanz-Canovas, J.; Lopez-Sampalo, A.; Hernandez-Negrin, H.; Perez-Velasco, M. A.; Perez-Belmonte, L. M.; Bernal-Lopez, M. R.; Gomez-Huelgas, R. Remission of type 2 diabetes: a critical appraisal. *Front. Endocrinol.* **2023**, *14*, No. 1125961.
- (8) Bennett, D. A.; Waters, M. D. Applying biomarker research. *Environ. Health Perspect.* **2000**, *108* (9), 907–910.
- (9) Li, Y.; Tam, W. W.; Yu, Y.; Zhuo, Z.; Xue, Z.; Tsang, C.; Qiao, X.; Wang, X.; Wang, W.; Li, Y.; et al. The application of aptamer in biomarker discovery. *Biomarker Res.* **2023**, *11* (1), No. 70.
- (10) Cawley, A. Biomarker analysis. *Drug Test. Anal.* **2022**, *14* (5), 791–793.
- (11) Li, K.; Tan, G.; Zhang, X.; Lu, W.; Ren, J.; Si, Y.; Adu-Gyamfi, E. A.; Li, F.; Wang, Y.; Xie, B.; Wang, M. Eif4g1 is a potential prognostic biomarker of breast cancer. *Biomolecules* **2022**, *12* (12), No. 1756.
- (12) Zheng, H.; Wang, M.; Zhang, S.; Hu, D.; Yang, Q.; Chen, M.; Zhang, X.; Zhang, Y.; Dai, J.; Liou, Y. C. Comprehensive pan-cancer analysis reveals nusap1 is a novel predictive biomarker for prognosis and immunotherapy response. *Int. J. Biol. Sci.* **2023**, *19* (14), 4689–4708.
- (13) Ashton, N. J.; Pascoal, T. A.; Karikari, T. K.; Benedet, A. L.; Lantero-Rodriguez, J.; Brinkmalm, G.; Snellman, A.; Scholl, M.; Troakes, C.; Hye, A.; et al. Plasma p-tau231: a new biomarker for incipient alzheimer's disease pathology. *Acta Neuropathol.* **2021**, *141* (5), 709–724.
- (14) Lees, T.; Nassif, N.; Simpson, A.; Shad-Kaneez, F.; Martiniello-Wilks, R.; Lin, Y.; Jones, A.; Qu, X.; Lal, S. Recent advances in molecular biomarkers for diabetes mellitus: a systematic review. *Biomarkers* **2017**, *22* (7), 604–613.
- (15) Tayek, C. J.; Cherukuri, L.; Hamal, S.; Tayek, J. A. Importance of fasting blood glucose goals in the management of type 2 diabetes mellitus: a review of the literature and a critical appraisal. *J. Diabetes Metab. Disord Control* **2018**, *5* (4), 113–117.
- (16) Ferrannini, G.; De Bacquer, D.; Gyberg, V.; De Backer, G.; Kotseva, K.; Mellbin, L. G.; Risebrink, R.; Tuomilehto, J.; Wood, D.; Ryden, L. Saving time by replacing the standardised two-hour oral glucose tolerance test with a one-hour test: validation of a new screening algorithm in patients with coronary artery disease from the esc-eorp euroaspire v registry. *Diabetes Res. Clin. Pract.* **2022**, *183*, No. 109156.
- (17) Zhao, H.; Qi, C.; Zheng, C.; Gan, K.; Ren, L.; Song, G. Effects of glycated hemoglobin level on bone metabolism biomarkers in patients with type 2 diabetes mellitus. *Diabetes, Metab. Syndr. Obes.: Targets Ther.* **2020**, *13*, 1785–1791.
- (18) Wang, Z.; Zhou, W.; Zhang, Z.; Zhang, L.; Li, M. Metformin alleviates spinal cord injury by inhibiting nerve cell ferroptosis through upregulation of heme oxygenase-1 expression. *Neural Regener. Res.* **2024**, *19* (9), 2041–2049.
- (19) Keane, K. N.; Calton, E. K.; Carlessi, R.; Hart, P. H.; Newsholme, P. The bioenergetics of inflammation: insights into obesity and type 2 diabetes. *Eur. J. Clin. Nutr.* **2017**, *71* (7), 904–912.
- (20) Liu, P.; Cao, B.; Zhou, Y.; Zhang, H.; Wang, C. Human umbilical cord-derived mesenchymal stem cells alleviate oxidative stress-induced islet impairment via the nrf2/ho-1 axis. *J. Mol. Cell Biol.* **2023**, *15* (5), No. mjad035, DOI: [10.1093/jmcb/mjad035](https://doi.org/10.1093/jmcb/mjad035).
- (21) Naito, Y.; Takagi, T.; Higashimura, Y. Heme oxygenase-1 and anti-inflammatory m2 macrophages. *Arch. Biochem. Biophys.* **2014**, *564*, 83–88.
- (22) Hong, J.; Kim, Y. H. Fatty liver/adipose tissue dual-targeting nanoparticles with heme oxygenase-1 inducer for amelioration of

obesity, obesity-induced type 2 diabetes, and steatohepatitis. *Adv. Sci.* **2022**, *9* (33), No. e2203286.

(23) Wei, Z.; Pinfang, K.; Jing, Z.; Zhuoya, Y.; Shaohuan, Q.; Chao, S. Curcumin improves diabetic cardiomyopathy by inhibiting pyroptosis through akt/nrf2/are pathway. *Mediators Inflammation* **2023**, *2023*, No. 3906043.

(24) Lenoir, O.; Gaillard, F.; Lazareth, H.; Robin, B.; Tharaux, P. L. Hmox1 deficiency sensitizes mice to peroxynitrite formation and diabetic glomerular microvascular injuries. *J. Diabetes Res.* **2017**, *2017*, No. 9603924.

(25) Chen, Q. Y.; Wang, G. G.; Li, W.; Jiang, Y. X.; Lu, X. H.; Zhou, P. P. Heme oxygenase-1 promotes delayed wound healing in diabetic rats. *J. Diabetes Res.* **2016**, *2016*, No. 9726503.

(26) Chen, L.; Du, S.; Li, Y. B.; Su, Q.; Zhang, J.; Zhang, H. Changes in serum tumor markers in type 2 diabetes mellitus with microalbuminuria. *Front. Endocrinol.* **2023**, *14*, No. 1247099.

(27) Sun, H.; Saeedi, P.; Karuranga, S.; Pinkepank, M.; Ogurtsova, K.; Duncan, B. B.; Stein, C.; Basit, A.; Chan, J.; Mbanya, J. C.; et al. Idf diabetes atlas: global, regional and country-level diabetes prevalence estimates for 2021 and projections for 2045. *Diabetes. Res. Clin. Pract.* **2022**, *183*, No. 109119.

(28) Ma, R. C. W. Epidemiology of diabetes and diabetic complications in china. *Diabetologia* **2018**, *61* (6), 1249–1260.

(29) Seo, H.; Park, J. H.; Hwang, J. T.; Choi, H. K.; Park, S. H.; Lee, J. Epigenetic profiling of type 2 diabetes mellitus: an epigenome-wide association study of dna methylation in the korean genome and epidemiology study. *Genes* **2023**, *14* (12), No. 2207.

(30) Wang, Z.; Ni, X.; Zhang, L.; Sun, L.; Zhu, X.; Zhou, Q.; Yang, Z.; Yuan, H. Toll-like receptor 4 and inflammatory micro-environment of pancreatic islets in type-2 diabetes mellitus: a therapeutic perspective. *Diabetes, Metab. Syndr. Targets Ther.* **2020**, *13*, 4261–4272.

(31) Lee, J. Adipose tissue macrophages in the development of obesity-induced inflammation, insulin resistance and type 2 diabetes. *Arch. Pharm. Res.* **2013**, *36* (2), 208–222.

(32) Wang, H.; Pan, F.; Liu, J.; Zhang, J.; Fuli, Z.; Wang, Y. Huayuwendan decoction ameliorates inflammation via il-17/nf-kappab signaling pathway in diabetic rats. *J. Ethnopharmacol.* **2024**, *319* (3), No. 117328.

(33) Meshkani, R.; Vakili, S. Tissue resident macrophages: key players in the pathogenesis of type 2 diabetes and its complications. *Clin. Chim. Acta* **2016**, *462*, 77–89.

(34) Cerf, M. E. Beta cell physiological dynamics and dysfunctional transitions in response to islet inflammation in obesity and diabetes. *Metabolites* **2020**, *10* (11), No. 452.

(35) Sánchez-Ortí, J. V.; Correa-Ghisays, P.; Balanza-Martinez, V.; Selva-Vera, G.; Vila-Frances, J.; Magdalena-Benedito, R.; San-Martin, C.; Victor, V. M.; Escribano-Lopez, I.; Hernandez-Mijares, A.; et al. Inflammation and lipid metabolism as potential biomarkers of memory impairment across type 2 diabetes mellitus and severe mental disorders. *Prog. Neuro-Psychopharmacol. Biol. Psychiatry* **2023**, *127*, No. 110817.

(36) Saltiel, A. R.; Olefsky, J. M. Inflammatory mechanisms linking obesity and metabolic disease. *J. Clin. Invest.* **2017**, *127* (1), 1–4.

(37) Saetang, J.; Sangkhathat, S. Role of innate lymphoid cells in obesity and metabolic disease (review). *Mol. Med. Rep.* **2017**, *17* (1), 1403–1412.

(38) Ying, W.; Fu, W.; Lee, Y. S.; Olefsky, J. M. The role of macrophages in obesity-associated islet inflammation and beta-cell abnormalities. *Nat. Rev. Endocrinol.* **2020**, *16* (2), 81–90.

(39) McLaughlin, T.; Ackerman, S. E.; Shen, L.; Engleman, E. Role of innate and adaptive immunity in obesity-associated metabolic disease. *J. Clin. Invest.* **2017**, *127* (1), 5–13.

(40) Tang, X.; Li, Y.; Zhao, J.; Liang, L.; Zhang, K.; Zhang, X.; Yu, H.; Du, H. Heme oxygenase-1 increases intracellular iron storage and suppresses inflammatory response of macrophages by inhibiting m1 polarization. *Metallomics* **2023**, *15* (10), No. mfa062.

(41) Hussein, M.; Wang, G. S.; Patrick, C.; Crookshank, J. A.; Macfarlane, A. J.; Noel, J. A.; Strom, A.; Scott, F. W. Heme oxygenase-

1 induction prevents autoimmune diabetes in association with pancreatic recruitment of m2-like macrophages, mesenchymal cells, and fibrocytes. *Endocrinology* **2015**, *156* (11), 3937–3949.

(42) Shen, X.; Yang, L.; Yan, S.; Zheng, H.; Liang, L.; Cai, X.; Liao, M. Fetuin a promotes lipotoxicity in beta cells through the tlr4 signaling pathway and the role of pioglitazone in anti-lipotoxicity. *Mol. Cell. Endocrinol.* **2015**, *412*, 1–11.

(43) Narayanankutty, A. Toll-like receptors as a novel therapeutic target for natural products against chronic diseases. *Curr. Drug Targets* **2019**, *20* (10), 1068–1080.

(44) He, M.; Qian, K.; Zhang, Y.; Huang, X. F.; Deng, C.; Zhang, B.; Gao, G.; Li, J.; Xie, H.; Sun, T. Olanzapine-induced activation of hypothalamic astrocytes and toll-like receptor-4 signaling via endoplasmic reticulum stress were related to olanzapine-induced weight gain. *Front. Neurosci.* **2021**, *14*, No. 589650.

(45) Yin, J.; Wang, H.; Lu, G. Umbelliferone alleviates hepatic injury in diabetic db/db mice via inhibiting inflammatory response and activating nrf2-mediated antioxidant. *Biosci. Rep.* **2018**, *38* (4), No. BSR20180444, DOI: 10.1042/BSR20180444.

(46) Kim, E. N.; Gao, M.; Choi, H.; Jeong, G. S. Marine microorganism-derived macrolactins inhibit inflammatory mediator effects in lps-induced macrophage and microglial cells by regulating bach1 and ho-1/nrf2 signals through inhibition of tlr4 activation. *Molecules* **2020**, *25* (3), No. 656.

(47) Vivot, K.; Langlois, A.; Bietiger, W.; Dal, S.; Seyfritz, E.; Pinget, M.; Jeandidier, N.; Maillard, E.; Gies, J. P.; Sigrist, S. Pro-inflammatory and pro-oxidant status of pancreatic islet in vitro is controlled by tlr-4 and ho-1 pathways. *PLoS One* **2014**, *9* (10), No. e107656.

(48) Tai, G. J.; Yu, Q. Q.; Li, J. P.; Wei, W.; Ji, X. M.; Zheng, R. F.; Li, X. X.; Wei, L.; Xu, M. Nlrp3 inflammasome links vascular senescence to diabetic vascular lesions. *Pharmacol. Res.* **2022**, *178*, No. 106143.

(49) Wei, W.; Li, X. X.; Xu, M. Inhibition of vascular neointima hyperplasia by fgf21 associated with fgfr1/syk/nlrp3 inflammasome pathway in diabetic mice. *Atherosclerosis* **2019**, *289*, 132–142.

(50) Ritchie, R. H.; Abel, E. D. Basic mechanisms of diabetic heart disease. *Circ. Res.* **2020**, *126* (11), 1501–1525.

(51) Tan, Y.; Zhang, Z.; Zheng, C.; Wintergerst, K. A.; Keller, B. B.; Cai, L. Mechanisms of diabetic cardiomyopathy and potential therapeutic strategies: preclinical and clinical evidence. *Nat. Rev. Cardiol.* **2020**, *17* (9), 585–607.

(52) Lu, C.; Fan, G.; Wang, D. Akebia saponin d ameliorated kidney injury and exerted anti-inflammatory and anti-apoptotic effects in diabetic nephropathy by activation of nrf2/ho-1 and inhibition of nf-kb pathway. *Int. Immunopharmacol.* **2020**, *84*, No. 106467.

(53) Chen, X.; Wang, H.; Zhou, M.; Li, X.; Fang, Z.; Gao, H.; Li, Y.; Hu, W. Valproic acid attenuates traumatic brain injury-induced inflammation in vivo: involvement of autophagy and the nrf2/are signaling pathway. *Front. Mol. Neurosci.* **2018**, *11*, No. 117.

(54) Matthews, D. R.; Paldanius, P. M.; Proot, P.; Chiang, Y.; Stumvoll, M.; Del, P. S. Glycaemic durability of an early combination therapy with vildagliptin and metformin versus sequential metformin monotherapy in newly diagnosed type 2 diabetes (verify): a 5-year, multicentre, randomised, double-blind trial. *Lancet* **2019**, *394* (10208), 1519–1529.